International Journal of the Physical Sciences Vol. 5(5), pp. 421-431, May 2010
Available online at http://www.academicjournals.org/IJPS
ISSN 1992 - 1950 © 2010 Academic Journals

Full Length Research Paper

Seismic refraction tomography of the periphery of an artificial lake in the Precambrian basement complex of Northern Nigeria

Chii E. Chii[1]* and I. B. Osazuwa[2]

[1]Department of Physics, Adamawa State University, Mubi, Nigeria.
[2]Department of Physics, Ahmadu Bello University, Zaria, Kaduna State, Nigeria.

Accepted 23 April, 2010

In order to investigate the subsurface seepage conditions of the Ahmadu Bello University (A. B. U.) farm dam, we have recorded high resolution seismic profiles spanning the entire periphery of the lake. Seismic waves generated from multiple shots were recorded on large number of closely spaced receivers using a 24 channel Abem Terraloc Mk 6 seismograph and the high-quality seismic data were processed using REFLEXW version 3.0 interpretation software. 2D seismic cross sections of the overburden and underlying bedrock were obtained and the physical composition of the subsurface materials was studied from their seismic velocity characteristics. On the basis of analysis of the data, the overburden shows evidence of unconsolidation with a seismic velocity range of 448 - 1875 m/s interpreted to represent lateritic clay material. The underlying bedrock shows evidence of differential weathering and saturation with a seismic velocity range of 1466 - 8061 m/s. Zones of relatively low seismic velocities within the bed rock are interpreted to represent zones of intense weathering and or fracturing and suspected to provide seepage pathway for water from the impounding reservoir.

Key words: Seismic refraction tomography, subsurface seepage condition, artificial lake, Nigeria.

INTRODUCTION

Inadequate preparation of the foundation and abutment of a dam before construction is one of the reasons for dam failure as the impounding reservoir might have defects in the form of weak zones associated with the geology of the area. Such defective zones might serve as anomalous seepage paths, making it difficult for the reservoir to store the intended volume of water and unable to serve its intended purpose.

Geophysical methods have the ability to detect anomalous seepage paths at an early stage before the integrity of the dam is at stake (e.g. Butler et al., 1989; Dahlin and Johansson, 1995; Sirles, 1997; Panthulu et al., 2001; Chen et al., 2004; Aal et al., 2009).

The A. B. U. farm dam, constructed in 1966, has no record of any geophysical survey carried out before its construction. This is blamed on the fact that engineering geophysics had not gain ground in the field of engineering (Butler et al., 1989) at the time the dam was constructed. However, a visual assessment of the embankment was carried out in 1977 and the property was declared to be at a state of dilapidation. Such dam inspection programs routinely identify deficiencies at dams, but inspections alone are inadequate to identify all the deficiencies because they are usually limited to the surface.

Recently, we have been involved in geophysical survey of the embankment and the flanks of the dam in which we systematically "scanned" the subsurface and identified anomalies of interest (Osazuwa and Chii, 2009; 2010). This work also aims at investigating the subsurface conditions around the periphery of the lake, using seismic refraction tomography, to detect weak zones favorable for seepage at the flanks of the dam. Such weak zones are usually products of weathering and or fracturing of the

*Corresponding author. E-mail: chiiemma@gmail.com.

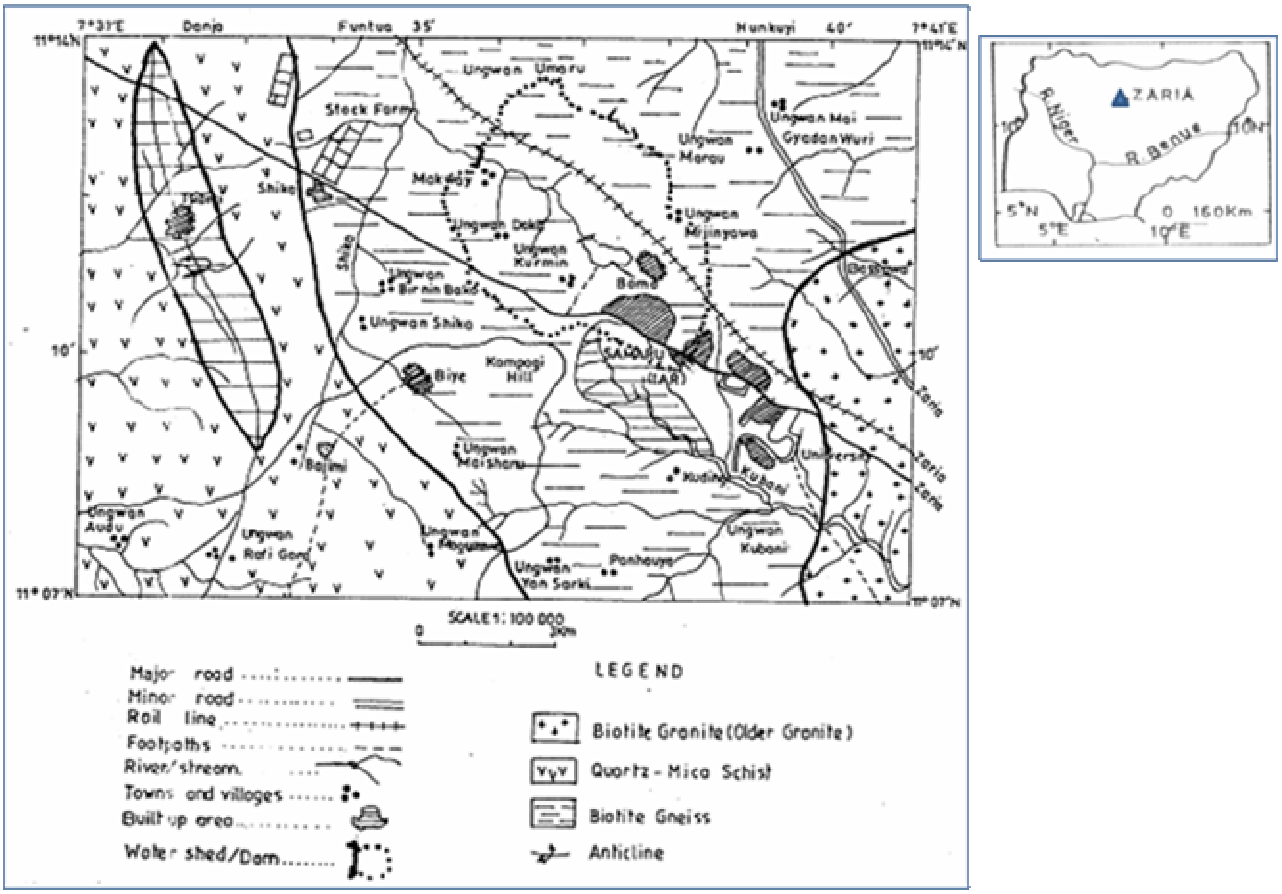

Figure 1. Geological map of the study area (McCurry, 1970).

bedrock which are identifiable as low velocity zones in a tomogram.

Physical environment, geology and hydrogeology of the study area

The Ahmadu Bello University Farm Dam is situated within the highly degraded former Guinea Savanna which has been mostly converted to farm land. The area has a typical Savannah climate of distinct wet and dry seasons, with a moderate rainfall of about 1047 mm/a. The rainy season usually starts in May and ends in October and the dry season last from late October to April (Walter, 1977).

The reservoir together with its drainage basin (19,247,000 m^2) is underlain by the biotite gneiss belonging to the Precambrian basement complex of northern Nigeria (Figure 1). It is therefore a metamorphic terrain bounded in the west by quartz-mica schist and in the east by biotite granite, believed to have intruded the basement gneiss during the Pan African Orogeny, according to McCurry (1970). The greater part of the area is covered with thick regolith mainly derived from in-situ weathering of the basement rocks. Some areas on the watershed are capped by lateritic material.

METHODOLOGY

The study involved a preliminary survey, followed by seismic refraction measurements and interpretation of the acquired data by using computer software in the laboratory. The preliminary work involved a number of tasks: Mapping the boundaries of the open water table of the impounding reservoir using satellite navigator; producing a map (Figure 2) showing the configuration of groundwater flow in the area and finally, selecting profile lines for the seismic refraction data acquisition.

The 2D seismic refraction method

High resolution seismic refraction data set were acquired on natural ground at the periphery of the impounding reservoir of the A.B.U. farm lake, along the profiles (P1, P2, P3, P4, P5, P6) shown in Figure 3. We used a sledge hammer and plate as source of our seismic waves with source locations spaced at 2.5m intervals. Geophones with natural frequencies of 10HZ spaced at 5m intervals were connected to a 24 channel Terraloc mk6 seismograph with source - receiver offset range of 0-30 m giving a profile length of 175m. Effective roll-along was achieved by shooting through the first 12 geophones of a receiver spread (that is one cable) and then moving the first cable to the end of the spread.

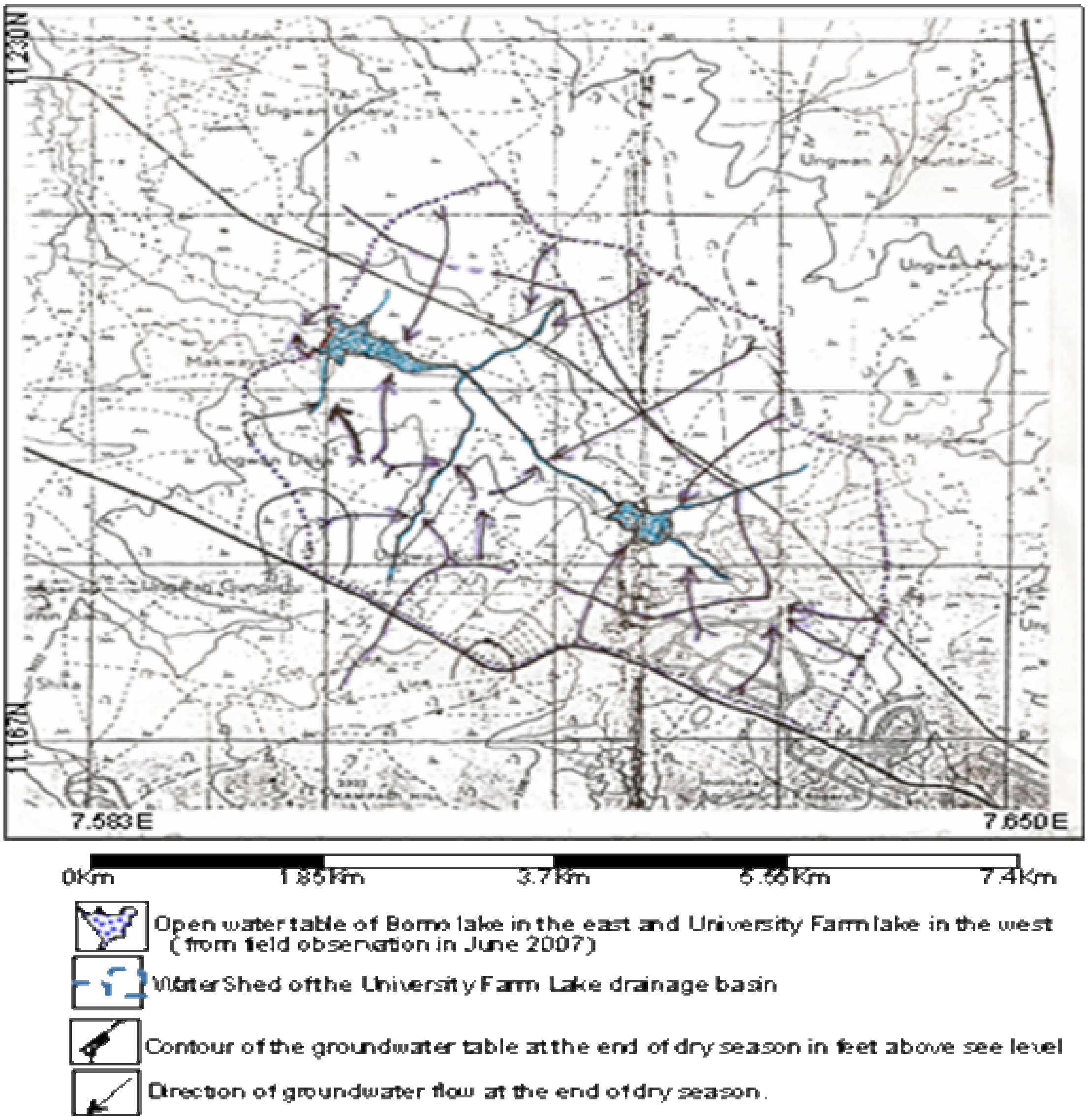

Figure 2. Map of configuration of groundwater table and directions of groundwater flow at the end of the dry season.

A total of 6,000 shots were required to complete the survey. Individual spreads were made to overlap in order that all parts of the refractor(s) beneath the profiles were directly sampled by critically refracted rays. Noise monitoring was carried out alongside data collection to make sure that the noise level was significantly reduced each time a set of data was collected. Five stacks were done per shot in order to further reduce the effect of noise thereby improving on the signal- to- noise ratio.

DATA ANALYSES

First-break picking

The data analysis was carried out using the seismic refraction module of Reflexw version 3.0 software by Sandmeier (2003). It is a versatile package that provides a wide range of processing and interpretation tools.

The raw data was first of all imported into the reflexw environment (Figure 4a shows a set of raw data traces for a shot point at 115m along profile 6). Unwanted signals were removed by using band pass filtering and the filtered signal enhanced using a gain function. Picking of the first- arrival was manually done (Figure 4b shows the enhanced signals with the first arrival picks (the red crosses)).

Traveltime processing

The traveltime processing module of the software provides the possibility of putting together the picked travel-times from all the shots along the profile (Figure 5 shows all picked travel times curves along profile 6) and assigning the picks to special layers (Figures 6a and b). The forward and reverse distance-time plots for each of the six spreads constituting the profile (of which Figure 6a is one of them) reveals a two layer case. The mean of the up- and down-tip

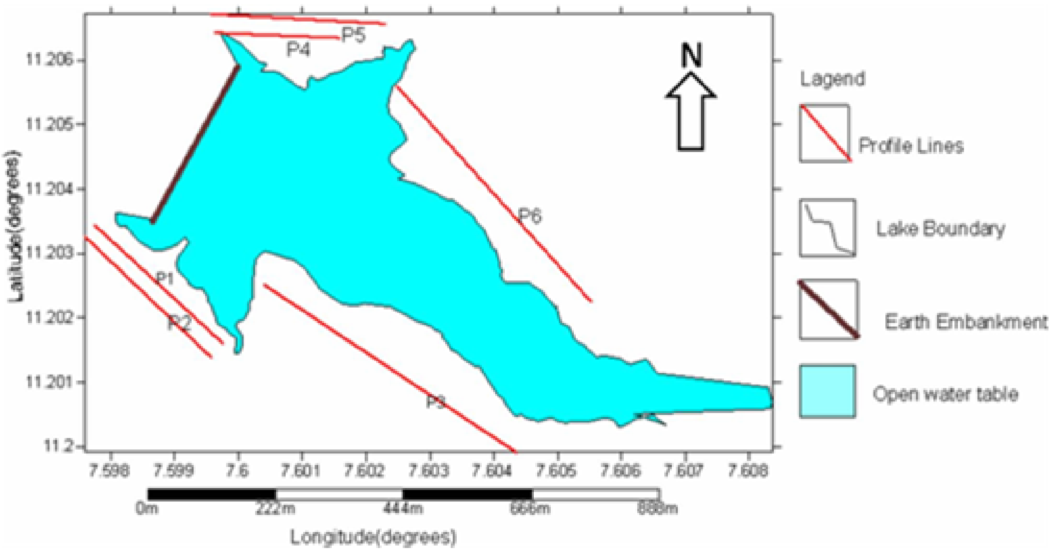

Figure 3. Location of profiles around the lake.

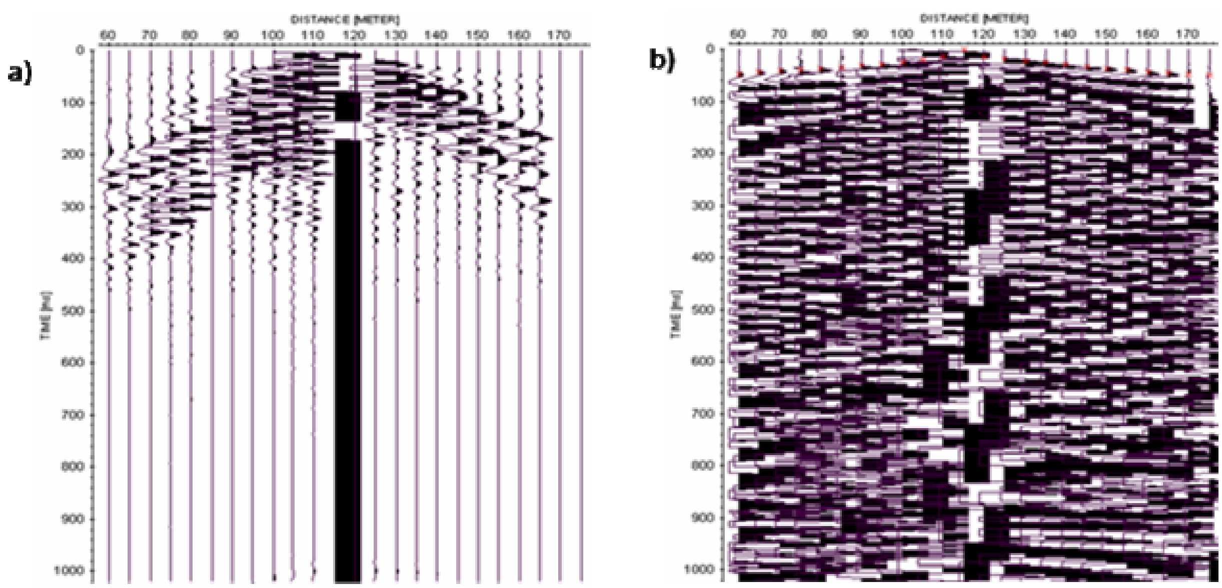

Figure 4. (a) Raw data and (b) Processed data showing picked first-arrival.

downdip traveltimes for the first layer was assigned to the first layer within that segment of the profile and so was the traveltimes assigned to the remaining segments constituting the entire profile. The green lines in figure 6b show the segments of the traveltime curves sampling the overburden while the blue are the segments sampling the basement.

Those traveltimes stemming from several shots and belonging to a particular layer were combined to one complete forward and reverse traveltime curves (Phantoming). Figure 6b shows the forward (red circle) and reverse (black circles) traveltime curves for the second layer. Analysis of the combined forward and reverse traveltimes shows a difference of 2.4151 (which is less than 5) indicating that the assignment of the traveltime to layers is accurate. These combined traveltimes are the basis for a subsequent 2D wavefront inversion.

Wave front inversion

After the phantoming, wavefront inversion was performed which enabled us to migrate the combined forward and reverse traveltimes into depth using a Finite Difference approximation of the eikonal equation, analogous to the forward raytracing by vidale (1988). We used model grids with spatial increment of 0.5. This value was chosen to avoid any significant loss of overburden inhomogeneity and also as a compromise between a good

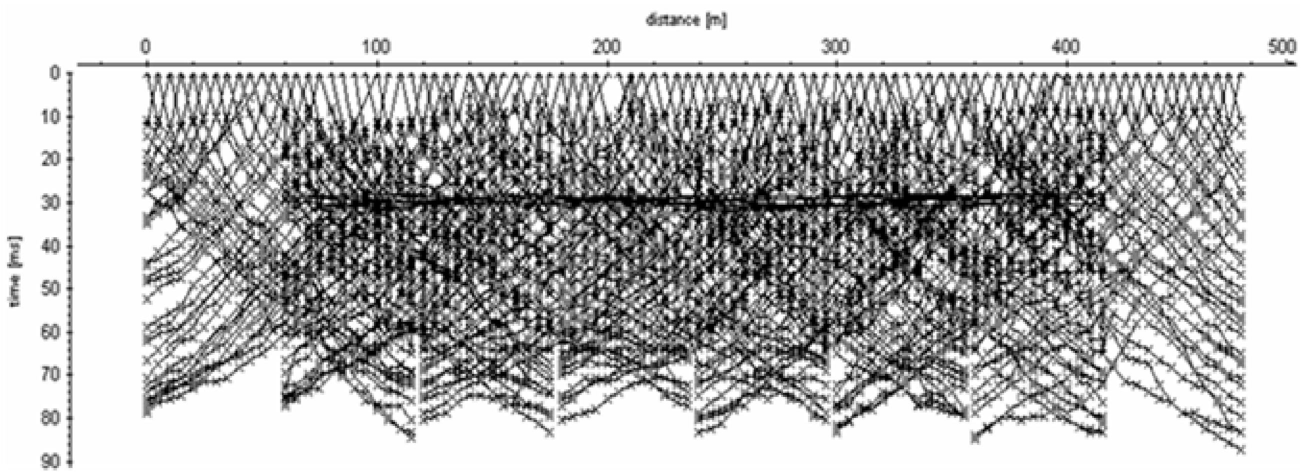

Figure 5. A combination of all the travel-times curves for all the shots along profile 6.

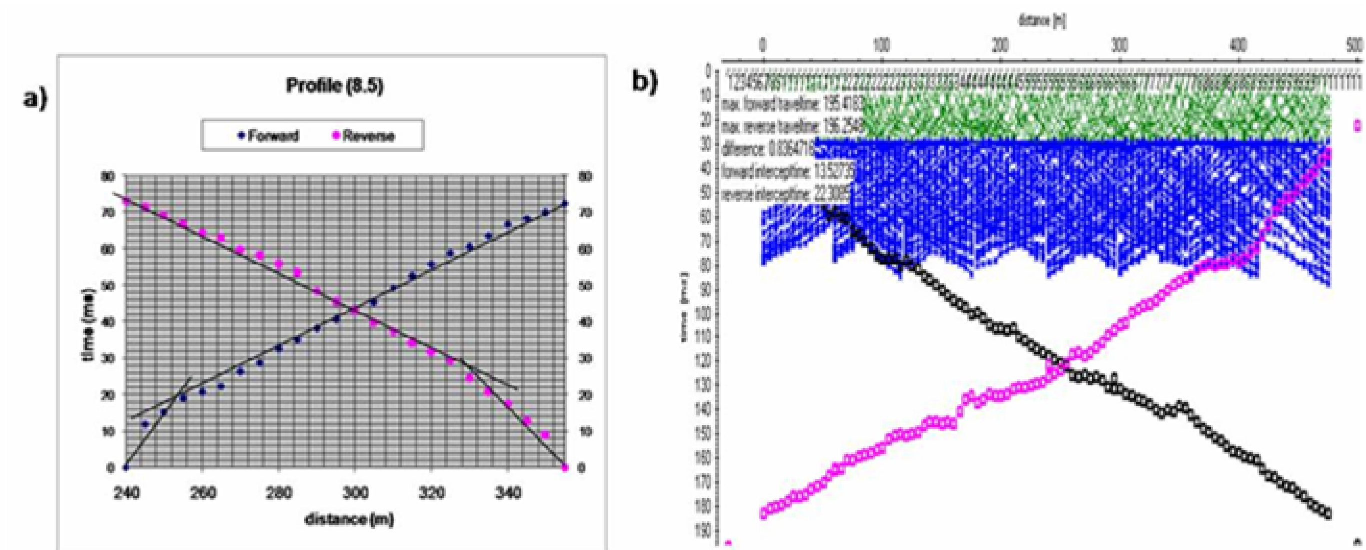

Figure 6. (a) One of six forward and reverse traveltime curves used for assignment of traveltime to layers. (b) Traveltime data put together and assigned to 2 different layers (the green represents the traveltimes segments corresponding to the first layer while the blue represents those for the second layer). For layer 2 one complete forward and reverse traveltime curve has been automatically generated (the red and black doted lines crossing each other).

resolution and cost in terms of computer time (computer time for the inversion increases by a factor of 4 if increment is decreased by a factor of 2).

The method is iterative, meaning that each layer must be inverted separately and that the overburden must be existent. For inverting the first layer, no overburden is necessary but to invert the second layer, the overburden must be known. When the option “wavefront-inversion” is activated for layer 1 the program automatically creates a new model consisting of the top layer boundary with layer points at the positions of the different traveltime branches assigned to layer 1. The velocities at these positions are automatically determined by linear regression.

For the second layer, the complete forward and reverse wavefronts are continued downward based on the given overburden model. The new refractor is automatically constructed at those points where the sum of the downward traveltimes is equal to the reciprocal traveltime. The refractor velocity is determined from the mean of the slopes of the forward and reverse wavefronts at the new calculated refractor points.

The end result of this process is interfaces of the layers and layer velocities which serve as initial model for subsequent tomographic inversion. Figure 7 shows the generated initial model, it is a two homogeneous layer case with overburden velocity of 630 m/s and the underlying layer of velocity of 3167 m/s.

Tomographic inversion

To determine the true subsurface velocities structure from the recorded traveltimes, the package uses a tomographic algorithm that simulates the propagation of wavefronts through complex 2d heterogeneous media thereby computing the raypaths and travel

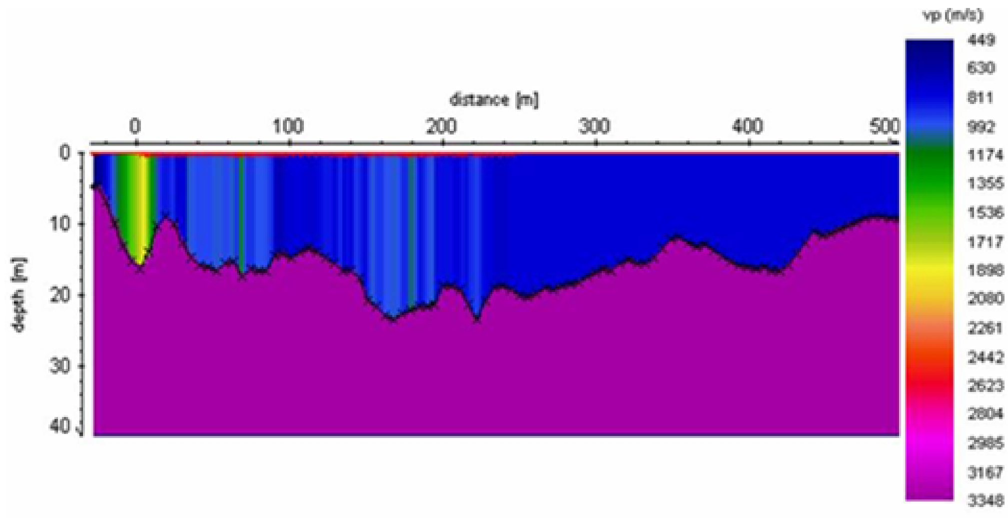

Figure 7. Initial model generated from wavefront inversion showing interface between the overburden and the underlying layer, serves as input model for tomographic inversion.

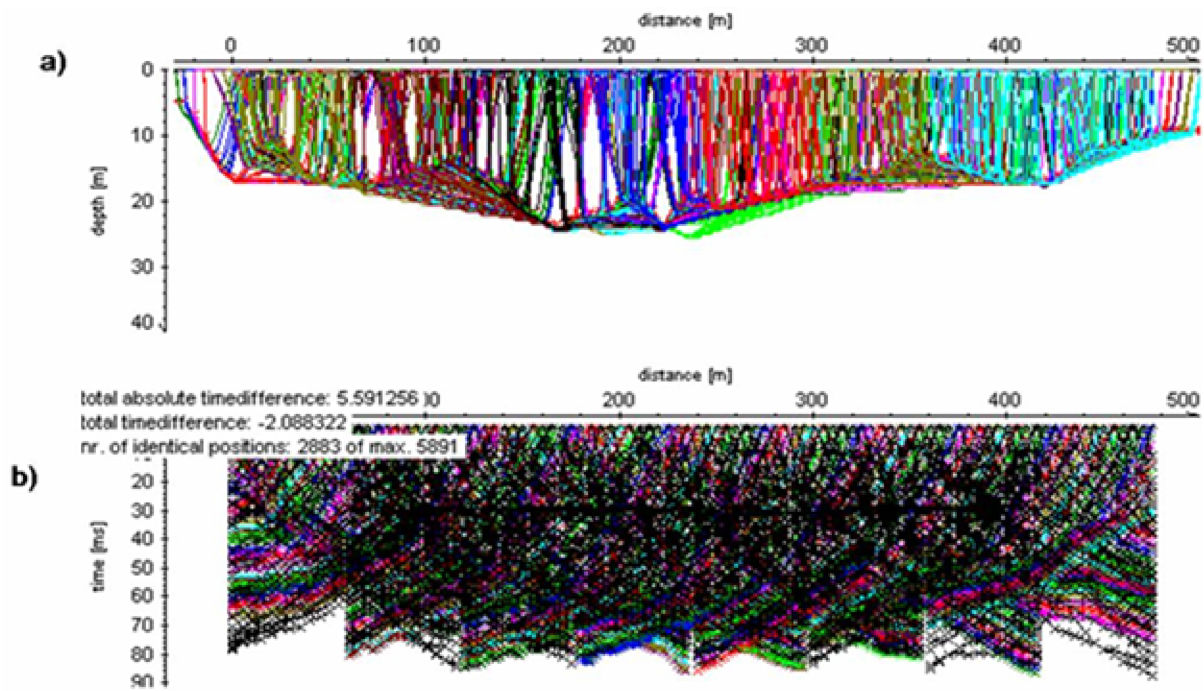

Figure 8. (a). Ray diagram and (b) Comparison of observed traveltimes (black) with the synthetic traveltimes based on tomographic result(Insert is the traveltime analysis showing total absolute timedifference of 5.591256 ms, total time difference of -2.088322 ms and number of identical positions of 2883).

times (Figure 8) by finite-difference approximation of the eikonal equation (Vidale, 1988).

The simulation technique allows the automatic adaptation of the synthetic traveltime data to real data based on a two-dimensional tomographic algorithm. The algorithm is based on, the Simultaneous Iterative Reconstruction Technique (SIRT). Starting from the initial model, the synthetic travel times are calculated using curved rays. These traveltimes are compared to the real (observed) ones and model changes (velocity distribution) are automatically derived from the travel time residuals. The procedure is repeated based on the changed model and stops when a distinct stopping criterion is fulfilled. In this case we used a stopping criterion of less than 2% model change and this was achieved after the 10th iteration. It takes into account the existence of different propagation waves like transmitted, diffracted or headwaves and therefore offers no practical limitation on the complexity of the medium. This makes

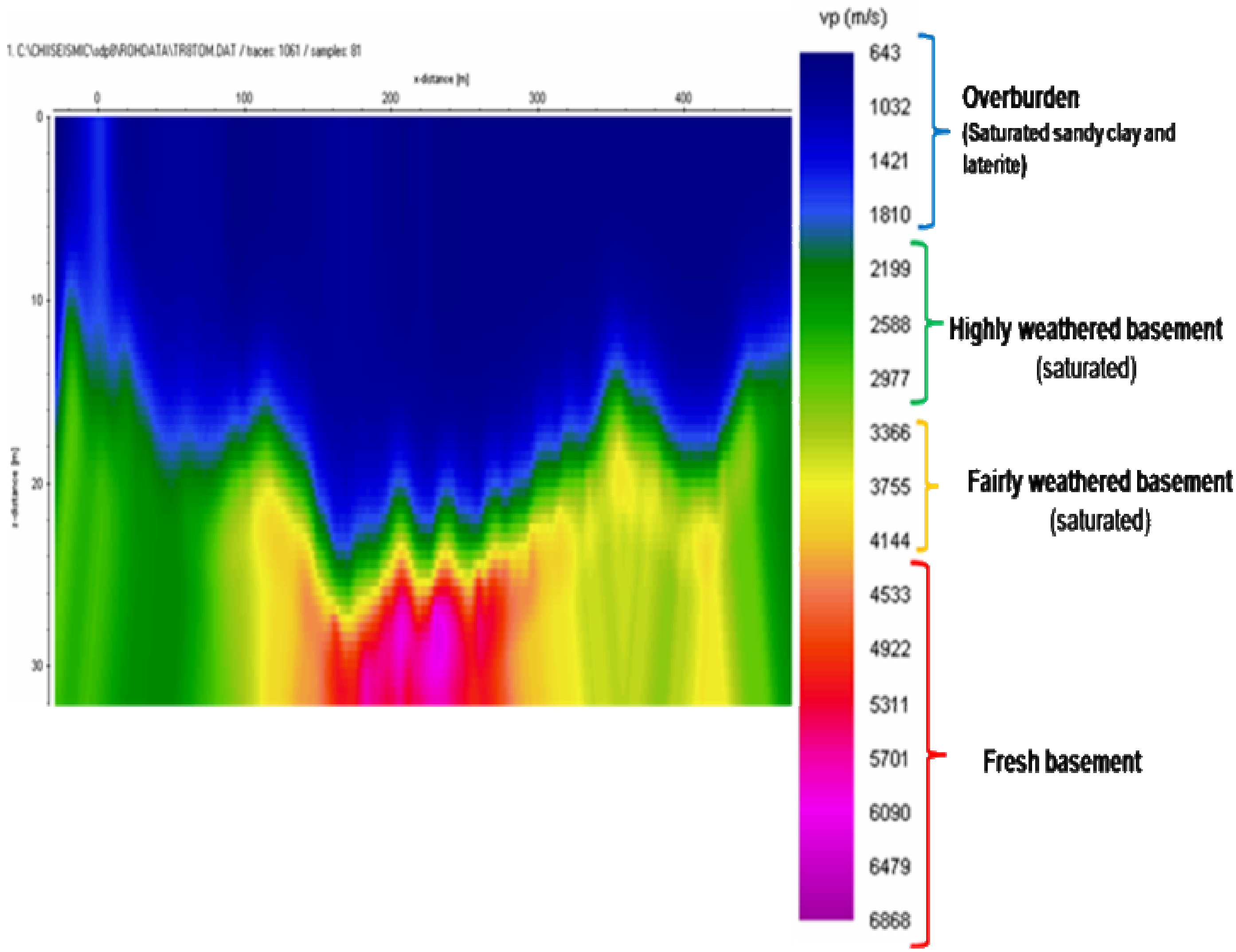

Figure 9. Final tomogram derived for profile 6 (P6) showing the full range of p-wave velocities between 643 and 6868 m/s with its geologic interpretation (Vertically exaggerated).

the method very suitable for near surface investigations of this nature since there is no need for approximation concerning the complexity of the model. The resulting velocity model is a rasterfile (tomogram) showing a range of velocities in colours (Figure 9).

RESULTS AND DISCUSSIONS

From the flow directions of water in the dam's drainage basin shown in Figure 2, it can be ascertain that the impounding reservoir is effluent with recharge favored through the flanks than seepage. This excludes the possibility of seepage taking place through loose grounds of the overburden which is usually a target anomaly in other seepage assessment projects. Thus any seepage along the flanks can most probably take place through deep seating weak zones (faults, joints, fractures, intensely weathered zones etc) within the bedrock all of which are detectable in a seismic refraction tomogram as velocity low within a frame work of velocity high.

The 6th profile (P6) was use to describe the procedure used in analyzing the seismic data. The same procedure applies to the other profiles investigated in this work.

Figure 9 shows the 2D tomographic inversion results for profile 6 with p-wave velocity range of 643- 6868m/s. Interpretation of the tomogram is guided with borehole log (Table 1) for the nearest borehole to the investigated area and standard p-wave velocities from other works in Table 2. The borehole was drilled in 2002 by the National Water Resource Institute (NWRI) to supply water to the Ahmadu Bello University Teaching Hospital, Student Hostel.

The ray diagram in Figure 8a provides information on the reliability of the tomogram. The dense nature of ray paths down to a depth of about 25 m indicates a high

Table 1. Lithology and aquifers borehole log (NWRI, 2002).

Depth (m)		Thickness (m)	Lithology
From	To		
0	15	15	Reddish brown laterite
15	21	6	Brownish sandy clay
21	42	21	Weathered basement
42	-	-	Fresh crystalline rock

Table 2. Standard P-wave velocities of soils and rocks (Keary and Brooks, 2002; Dobrin, 1976; Osemeikhian and Asokhia, 1994).

Material	P-wave velocity (m/s)
Air	300-330
Water	1400-1800
Alluvium sand (dry)	300-1000
Sand (water-saturated)	1200-2000
clay	1100-2500
Granite and gneiss	2000-6200

resolution of the overburden. Ray coverage and therefore confidence in velocity estimates is reduced at depth greater than 25m below the surface.

Figure 8b show how well the synthetic and observed traveltimes match. The traveltime analysis shows: total absolute time difference, between the synthetic and observed, of 5.591256 ms; total time difference of -2.088322 ms and number of identical positions of 2883 out of 5891. This further emphasizes the reliability of the final tomographic inversion result.

It is well known that seismic velocity is a function of the density and elastic properties of the rock materials. It was therefore taken into consideration that variations in velocity in a localized work of this natures is as a result of variation in densities, most probably, associated with variation in the extent of weathering and or saturation than a variation of rock type. For example, P-wave velocity changes dramatically from dry alluvium to saturated alluvium because the p-wave energy can propagate both through the matrix of alluvium and through the interstitial water. The seismic sections are therefore interpreted as follows:

For the 6th profile used as an example to illustrate the steps in the data analysis, the final tomogram derived for this profile and presented in Figure 9 comprises of a top layer with velocity 643 – 1810 m/s and thickness of about 10 – 23 m is interpreted to represent the overburden which composes of saturated sandy clay and laterite. This is underlain by the gneissic bedrock showing a lateral variation in velocity from 2199-6868 m/s. This is subdivided into:

(1) The highly weathered basement with velocity range 2199-2977m/s

(2) The fairly weathered basement of velocity range of 3366 – 4144 m/s and finally

(3) The fresh basement of velocity range of 4533 - 6868 m/s.

Similarly, the remaining profiles are interpreted as shown in Figures 10 - 14.

In regards to the aim of this work which is to detect weak zones within the bedrock that are potential seepage paths of water from the impounding reservoir, P1, P3, P4, and P5 shows anomalies of interest .

P1(Figure 10) shows evidence of a weak zone of average velocity 2975 m/s, flanked by zones of high velocity ranging from 4909 - 6840 m/s. The zone is centered at 190 m along the profile and occurs at a depth of about 28 m extending downward to the depth of investigation. It has width of about 6m and such a low velocity zone (weak zone) within a high velocity framework could serve as a pathway for seepage from the reservoir. This also applies to the weak zone identified in P3, P4, and P5.

The seemingly weak zones at the edges of the tomograms are considered to be associated with edge effect linked with the data analysis.

ACKNOWLEDGEMENTS

We wish to acknowledge the International Programme in the Physical Sciences (IPPS) Uppsala University Sweden for providing the equipments used in this work and part of the funding. Also, my gratitude to Professor Osazuwa I. B. of the department of physics, Ahmadu Bello University, Zaria, Nigeria and to Professor K. Schoeneich, of the Department of Geology of the same university, for closely supervising the work.

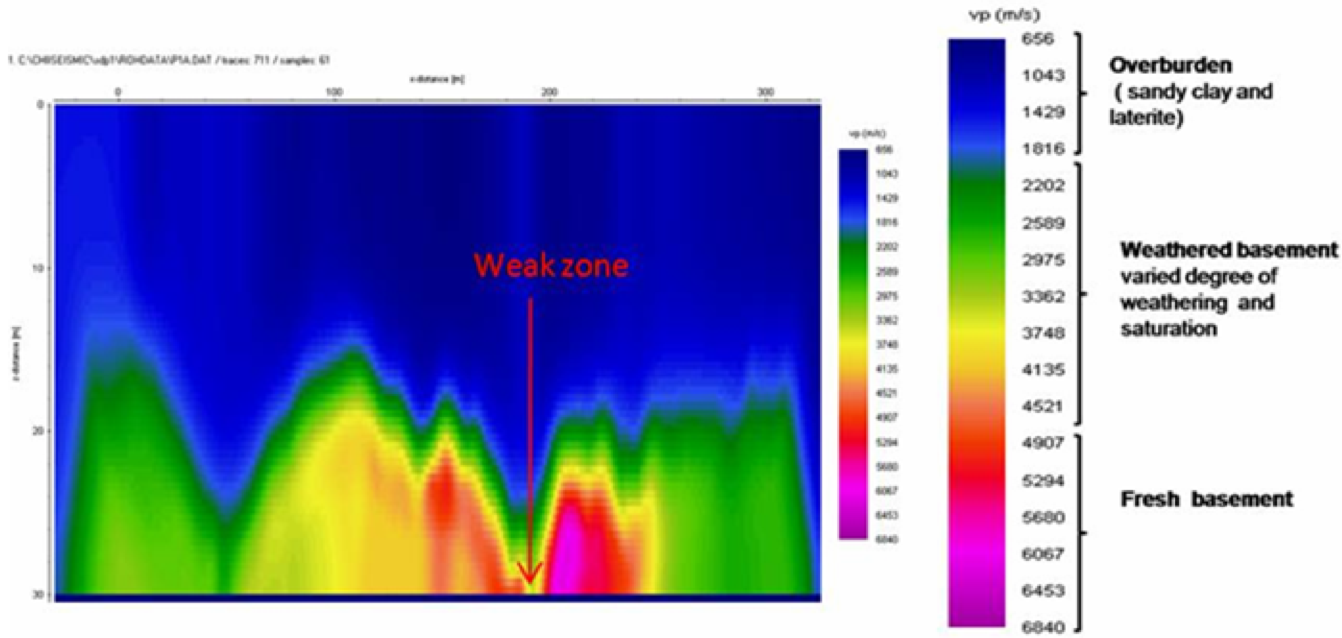

Figure 10. Seismic tomogram for profile one with its geologic interpretation.

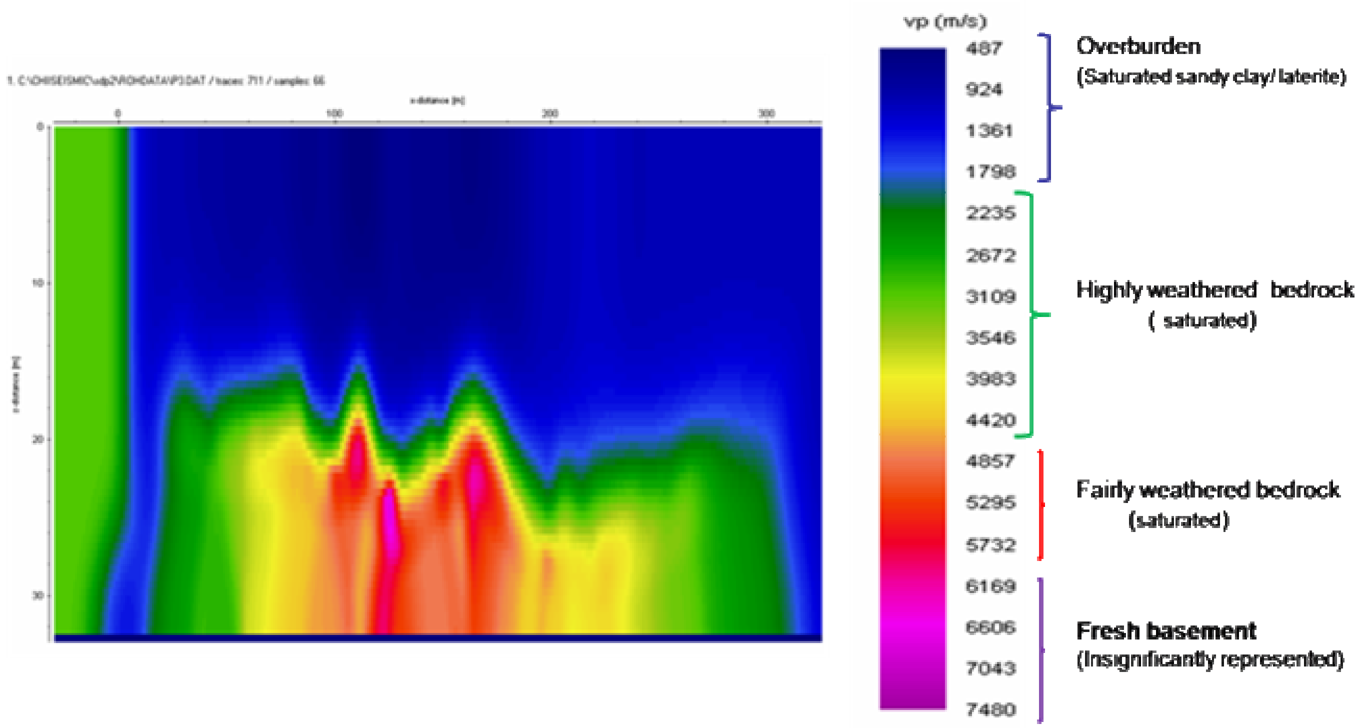

Figure 11. Seismic tomogram for profile two with its geologic interpretation.

Conclusion

An essential requirement for the successful application of surface-based tomographic refraction method is a high quality traveltime data set. Such a data quality was achieved through noise monitoring, stacking and deployment of large number of closely spaced receivers.

To process and interpret the comprehensive travel time

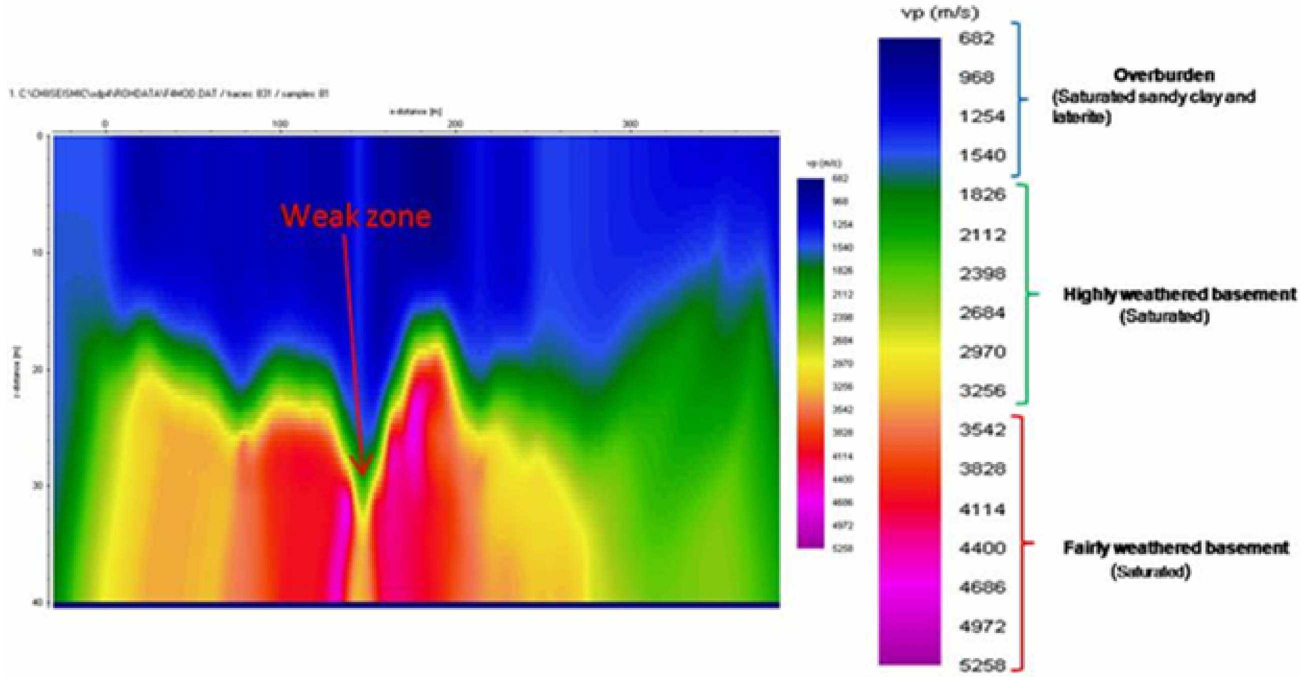

Figure 12. Seismic tomogram for profile three with its geologic interpretation.

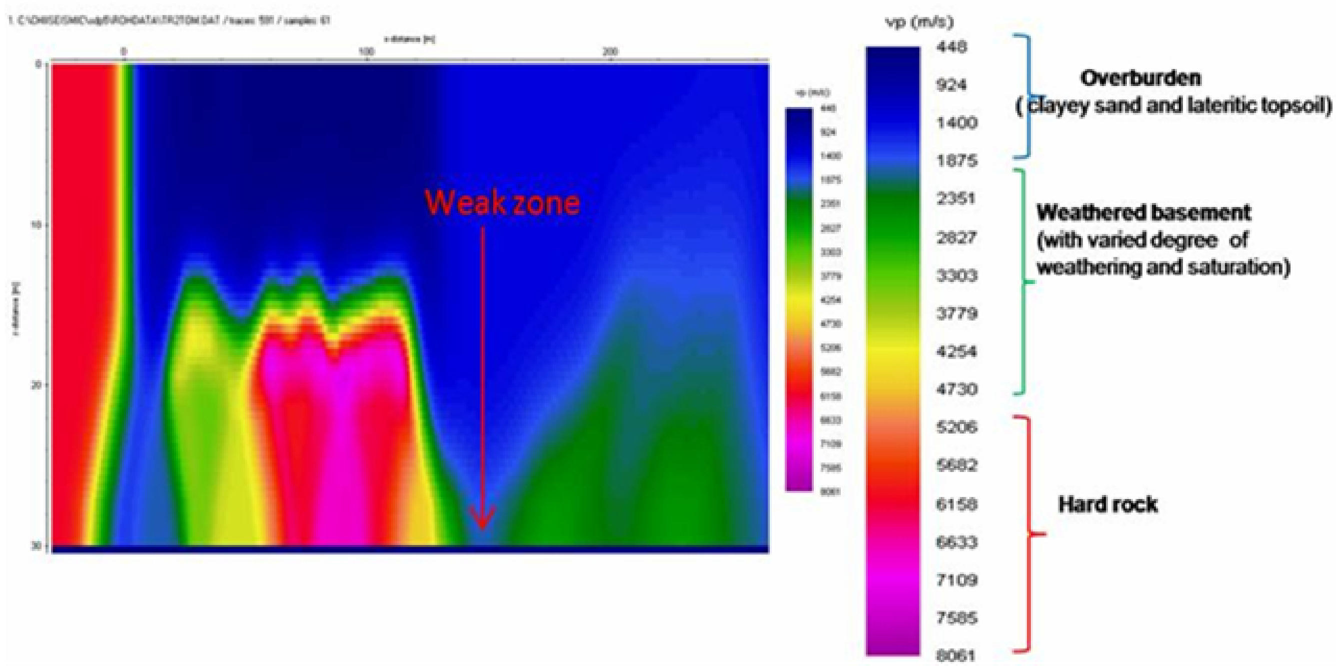

Figure 13. Seismic tomogram for profile four with its geologic interpretation.

data set, we used a tomographic refraction scheme based on finite – difference eikonal solver and an inversion method that incorporates both damping and smoothness constraints. An essential component of this work was to ensure that the computed tomogram was reliable and of good quality. We achieved this goal by matching details on the tomograms with the appropriate ray diagrams and plotting together the synthetic and

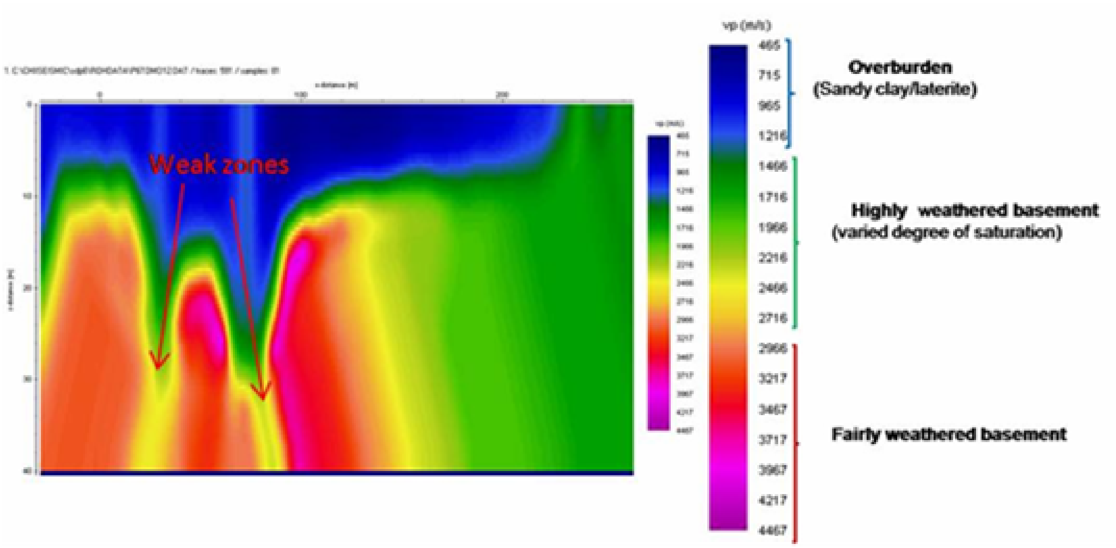

Figure 14. Seismic tomogram for profile five with its geologic interpretation.

observed travel times.

According to the results of this survey the subsurface geology of the area could be summarized as follows:

1. A surface layer of variable thickness ranging from 6 – 28 m composed of unconsolidated sandy clay and laterite, generally saturated and is characterized by low seismic velocities ranging from 448 – 1875 m/s.
2. A second layer which is usually the weathered basement with moderate velocity of 1041 - 5732 m/s. This is further subdivided into highly and fairly weathered basement depending on the seismic velocity values. The depth to this layer varies from 6 - 28 m.
3. The last layer which is the fresh basement with high seismic velocity was not encountered in most of the tomogram except in a few where they could be attributed to artifacts.

Defective zones have been identified within the bedrock, beneath most of the profiles investigated, at the periphery of the lake as zones of weakness with relatively low p-wave velocity compared with the surrounding rock. These weak zones have been indicated in the velocity tomograms, using arrows in Figures 10, 12, 13 and 14. This probably contributes to the inability of the reservoir to be filled to capacity for a greater part of the year.

We are recommending that the defective zones identified be repaired by injection grouting. This involves drilling at those locations and pumping a mixture of cement and water under high pressure.

REFERENCES

Aal Gamal Z, Abdel Ahmed M, Ismail Neil L, Anderson Estella A, Atekwana (2009). Geophysical Investigation of Seepage from an Earth Fill Dam, Washington County, Mo. www.dot.state.fl.us

Butler KD, LLopis LJ, Deaver MC (1989). Comprehensive geophysical investigation of an existing dam foundation, The leading Edge of Exploration , pp. 10-18.

Chen C, Xia J, Chen J, Lin W (2004). Detection of potential leak sites in embankments using surface-wave method and electrical method. Procs. SEG International Exposition and 74th Annual Meeting, Denver, USA, 4: 10-15.

Dahlin T, Johansson S (1995). Resistivity Variation in an Earth Embankment Dam in Sweden. Procs Torino, Italy. 1st Meeting Environ Eng Geophy,pp. 25-27

Dobrin MB(1976). Introduction to Geophysical Prospecting. McGraw-Hill, Pp 50,630.

Keary P, Brooks M (2002). An Introduction to Geophysical Exploration. Blackwell. 255 p.

McCurry P (1970). The Geology of Degree Sheet 21 Zaria. Unpublished MSc. Theses, A.B.U. Zaria.

Osazuwa IB, Chii EC (2009). A two-dimensional electrical resistivity imaging of an earth dam, zaria nigeria. J. Environ. Hydrol. Vol. 17 paper 28 October 2009, published by the International Association for Environmental Hydrology on the World Wide Web at http://www.hydroweb.com.

Osazuwa IB, Chii EC (2010). Two-dimensional electrical resistivity survey around the periphery of an artificial lake in the Precambrian basement complex of northern Nigeria. Inter. J. Phys. Sci, 5(3): 238-245. March 2010 Available online at http://www.academicjournals.org/IJPS

Osemeikhain JEA, Asokhia MB (1994). Applied Geophysics For Engineers and Geologist. 120.

Panthulu TV, Krishnaiah C, Shirke JM (2001). Detection of seepage paths in earth dams using self-potential and electrical resistivity methods. Eng. Geol, 59: 281-295.

Sandmeier KJ (2003). Windows™ 9x/NT/2000/XP-program for the processing of seismic, acoustic or electromagnetic reflection, refraction and transmission data, Manual for REFLEXW, Version 3.0, p177,(available at www.sandmeier-geo.de).

Sirles P (1997). Seepage investigation using geophysical techniques at Coursier Lake Dam BC, Canada. Symposium of the Geophysical Application to Environmental and Engineering Problems (SAGGEP), Reno-Nevada, 1: 321-331.

Vidale J (1988). Finite-difference calculation of travel time Bullettin of the Seismological Society of America, 78(6): 2062-2076.

Walter MW (1977). The Length of the Rainy Season in Nigeria. Agric Meteorol, p.18.